International Journal of Materials Science ISSN 0973-4589 Volume 12, Number 2 (2017)


# Spectroscopic (FT-IR, FT Raman) and Quantum Mechanical Study on Isosorbide Mononitrate by Density Functional Theory.

**Jacob George[1], Johanan Christian Prasana[1], S. Muthu[2*], Tintu K. Kuruvilla[1]**

[1]*Department of Physics, Madras Christian College, East Tambaram 600059, Tamil Nadu, India,*

[2] *Department of Physics, Arignar Anna Government Arts College, Cheyyar, 604407, Tamil Nadu, India.*

**E-mail:* mutgee@gmail.com

## ABSTRACT

Quantum chemical techniques like the DFT have become a key tool in the analysis of molecular structure and vibrational spectrum and are finding widespread use in the applications related to biological systems. Experimental and theoretical investigations on the molecular structure, electronic and vibrational characteristics of Isosorbide Mononitrate are presented in this work. DFT/B3LYP calculations were used to obtain the vibrational frequencies using 6-311++G (d,p) basis set. This was compared with experimental FT-IR and FT-Raman spectral data and was in good agreement with the simulated spectra. The complete optimization of the molecular equilibrium geometry of the title compound was carried out. Quantum chemical calculations of the equilibrium geometry and the complete vibrational assignments of wavenumbers using potential energy distribution (PED) were calculated using the VEDA software. HOMO-LUMO has been calculated using the DFT method. Energy gap (ΔE), electronegativity (χ), chemical potential (μ), global hardness (η), softness (S) and the Fukui function were calculated for the title molecule. The stability and charge delocalization of the title molecule were studied by Natural Bond Orbital (NBO) analysis, Non Linear Optical (NLO) behavior in terms of first order hyperpolarizability, dipole moment and anisotropy of polarizability and Molecular Electrostatic Potential (MEP) were calculated. Thermodynamic properties of the title molecule were studied and the correlations between heat capacity (*C*), entropy (*S*) and enthalpy changes (*H*) with temperatures were analyzed. The charge distribution has been studied with the help of Mulliken population analysis.

**Keywords:** DFT; FT-IR; FT-Raman; HOMO-LUMO; Vasodilator; NBO Analysis.

## 1. INTRODUCTION

Isosorbide mononitrate ($C_6H_9NO_6$) is a drug used primarily in the treatment of angina pectoris and acts by dilating the blood vessels so as to reduce the blood pressure. It is sold by AstraZeneca under the trade name Imdur. Isosorbide mononitrate is the key for the prophylactic cure of angina pectoris; to prevent or at least reduce the occurrence of angina[1-2]. Investigation on Isosorbide mononitrate as a cervical ripener (during birth) is also underway[3]. Isosorbide mononitrate is a key metabolite of isosorbide dinitrate and has similar effects[4]. Isosorbide mononitrate diminishes the workload of the heart by creating the venous and arterial dilation. It lowers intramural pressure by reducing the end diastolic pressure and volume leading to an improvement in the subendocardial blood flow[5-6]. When administered, Isosorbide mononitrate reduces workload of the heart and improves oxygen supply and balance of the myocardium. It is also used to prevent Isosorbide Mononitrate to check recurring variceal bleeding[7].

Literature survey reveals that so far there are no detailed spectroscopic and theoretical studies on the title compound. In this present study, a detailed spectroscopic approach of Isosorbide mononitrate is reported using B3LYP/6-311++G(d,p) level of the theory. Molecular properties like dipole moment, polarizability, and first order hyperpolarizability, molecular electrostatic potential and thermodynamic parameters have been calculated for the title compound. The frontier molecular orbitals such as HOMO and LUMO determine the way the molecule interacts with other species which enable us to characterize the chemical reactivity of the molecule. The natural bond orbital (NBO) analysis has been applied to analyze the stability of molecule arising from hyper conjugative interaction and charge delocalization. In addition the thermodynamic properties were also calculated.

## 2. EXPERIMENTAL

Solid form of Isosorbide Mononitrate purchased from Sigma-Aldrich Chemical Company(USA), with a purity of more than 98% was used without any further purification. The FT-IR spectrum of the compound was recorded in the region between 4000 $cm^{-1}$ and 450 $cm^{-1}$ in SAIF IIT Chennai, India, using KBr pellet technique on Perkin Elmer Spectrum1 spectrometer. The FT-Raman spectrum for the sample was recorded in the region 4000 $cm^{-1}$ to 50 $cm^{-1}$ using Nd:Yag laser 1064nm on Bruker RFS 27 spectrophotometer at SAIF, IIT Chennai, India.

## 3. COMPUTATIONAL DETAILS

The complete set of theoretical calculations was carried out with DFT method Gaussian software package [8]. Optimized molecular structure, vibrational spectra, molecular electrostatic potential, were calculated using the B3LYP function with 6-311++G(d,p) as the basis set. A scaling factor of 0.960 above 3000 $cm^{-1}$ and 0.961 below 3000 $cm^{-1}$ were applied to the calculated harmonic vibrational frequency calculations for B3LYP/6-311++G(d,p) [9,10]. Potential Energy Distribution (PED) analysis was carried out for the entire set of fundamental modes of vibration using the VEDA 4 program in order to explain the calculated vibrational frequencies [11],

which is a widely used method [12-14]. The experimental and theoretical IR and Raman spectrums were compared with the help of Origin and Gabedit software.
Chemcraft (graphical software) was used to generate the molecular structure with the numbering scheme for atoms and the geometrical parameters (Bond length and Bond Angle). Properties like first order hyperpolarizability, dipole moment, anisotropy of polarisability of Isosorbide mononitrate were calculated theoretically using the basis set 6-311++G(d,p) at B3LYP level in order to understand the non linear optical behavior of the compound. Highest occupied molecular orbital (HOMO) and lowest unoccupied Molecular orbital (LUMO) energies were determined so that the way in which the molecule interacts with other species can be determined. Surface mapping based on the electrostatic potential was done for the title compound using Gauss View software [15]. The Natural Bond Analysis (NBO) [16] was carried out for the title compound with 6-311++G(d,p) basis set using B3LYP level to provide a clear evidence of stabilization originating from hyper conjugation of different intramolecular interactions**.**

## 4. RESULTS AND DISCUSSIONS

### *4.1 Molecular Geometry*

The DFT method in conjunction with the basis set B3LYP/6-311++G(d,p) was used to calculate the optimized structure parameters for Isosorbide mononitrate and have been listed in Table1 in accordance with the numbering scheme shown in Fig.1.

A crystal system which is structurally similar to the title compound, whose crystal structure has been solved, was taken to compare the results with the obtained optimized structure as the exact crystal structure of the title compound was not available.

An X-ray study of the a dioxaphosphorinane compound, which contains a nitro group and two fused oxolane rings, having similar structure to that of the title compound has been selected as the experimental data [17,18]. The small deviation found between the experimental and theoretical geometry can be due to the fact that theoretical calculations were carried out on a free molecule, neglecting the intermolecular and intramolecular interactions which are prevalent in the solid form. The highest bond length was found to be C1-C5(1.54Å). The deviation between the experimental and theoretical bond length was found to be lesser than 0.05 Å except for the one between C3-C4 and C5-O6. The homonuclear bond lengths were found to be greater than hectronuclear bond length, the reason being that same charges repel but opposite charges attract. The deviation between the experimental and theoretical bond angles were found to be with the range 0.2º-6 º. Hence the reliability criterions of the calculated structural parameter were more or less satisfied [19].

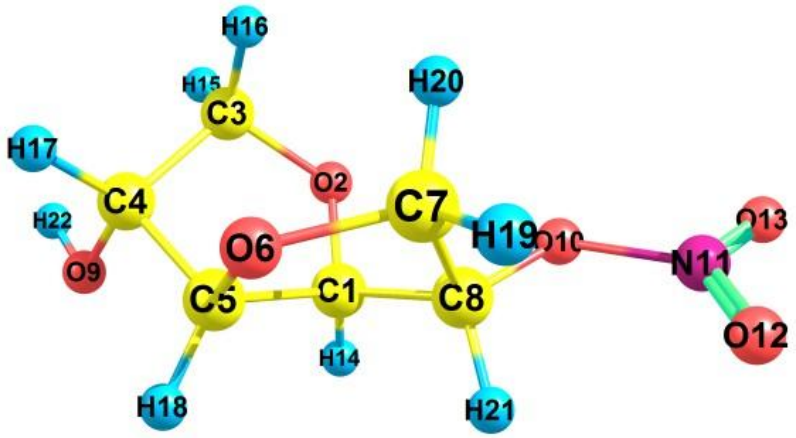


Fig 1: Numbering scheme for the optimized molecular structure of Isosorbide Mononitrate.

Table 1: Selected optimized parameters of Isosorbide Mononitrate {Bond Length (Å) and Bond Angle(°)}

| ***Bond Length(Å)*** | **B3LYP/6-311++G(d,p)** | **Experimental*** | ***Bond Angle(°)*** | **B3LYP/6-311++G(d,p)** | **Experimental*** |
|---|---|---|---|---|---|
| $C_1$-$O_2$ | 1.42 | 1.42 | $O_2$-$C_1$-$C_5$ | 106.7 | 110 |
| $C_1$-$C_5$ | 1.54 | 1.53 | $O_2$-$C_1$-$C_8$ | 112.4 | 112.8 |
| $C_1$-$C_8$ | 1.54 | 1.52 | $O_2$-$C_1$-$H_{14}$ | 109.1 | - |
| $O_2$-$C_3$ | 1.44 | 1.43 | $C_1$-$O_2$-$C_3$ | 110.8 | 109.1 |
| $C_3$-$C_4$ | 1.52 | 1.44 | $C_1$-$C_5$-$O_6$ | 106.9 | 109 |
| $C_4$-$C_5$ | 1.54 | 1.56 | $C_1$-$C_8$-$O_{10}$ | 108.8 | 109 |
| $C_4$-$O_9$ | 1.43 | 1.42 | $O_2$-$C_3$-$C_4$ | 106.4 | 109.1 |
| $C_5$-$O_6$ | 1.44 | 1.33 | $O_2$-$C_3$-$H_{16}$ | 109.9 | - |
| $O_6$-$C_7$ | 1.43 | 1.41 | $C_3$-$C_4$-$O_9$ | 108.3 | 108.5 |
| $C_7$-$C_8$ | 1.53 | 1.51 | $C_5$-$C_4$-$O_9$ | 111.1 | 113.3 |
| $C_8$-$O_{10}$ | 1.44 | 1.46 | $O_9$-$C_4$-$H_{17}$ | 111.7 | - |
| $O_{12}$ -$N_{11}$ | 1.43 | 1.41 | $O_6$-$C_5$-$H_{18}$ | 108.7 | - |
| $N_{11}$-$O_{12}$ | 1.21 | 1.23 | $C_5$-$O_6$-$C_7$ | 110.6 | 112.8 |
| $N_{11}$-$O_{13}$ | 1.2 | 1.2 | $O_6$-$C_7$-$C_8$ | 104 | 110 |
| | | | $O_6$-$C_7$-$H_{20}$ | 111.3 | - |
| | | | $C_7$-$C_8$-$O_{10}$ | 115.3 | 113.3 |
| | | | $O_{12}$-$N_{11}$-$_{13}$ | 129.9 | 128 |

*Taken from Ref. [17,18]

## *4.2 Vibrational Analysis*

The title compound Isosorbide mononitrate has 22 atoms and hence has 60 normal modes of vibration. The small discrepancies in the experimental and theoretical vibrational wave numbers points to the fact that the theoretical calculation were made for a free molecule in vacuum but the experimental analysis was carried out for the sample in solid form. Table 2 gives the theoretical (unscaled, scaled) and experimental frequencies. The absolute intensity for each frequency is the percentage of the ratio between the corresponding relative intensity and the peak value of the relative intensity. Theoretical and experimental graphs of both FT-IR and FT Raman are given in Fig 2 and Fig 3 respectively. The Potential energy distribution was calculated and the vibrational assignments have been made with the help of VEDA software.

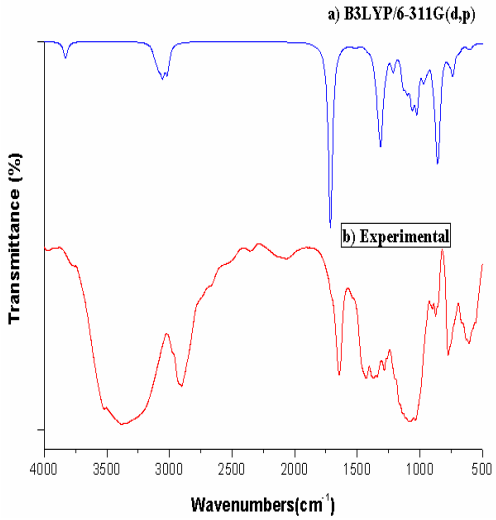


Fig 2: Theoretical and experimental FT-IR.

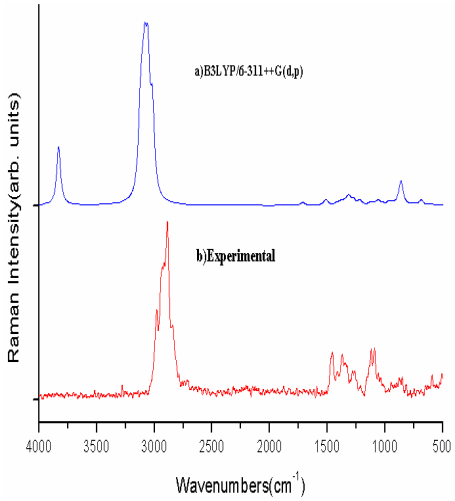


Fig 3: Theoretical and experimental FT-Raman

Table 2: Calculated and vibrational wavenumber, measured IR and Raman band position ($cm^{-1}$) and assignments of Isosorbide Mononitrate

| MODE | Frequencies($cm^{-1}$) | | | | IR Intensity | | Raman Activity | | Vibrational Assignments(%PED) |
|---|---|---|---|---|---|---|---|---|---|
| | Experimental | | Theoretical | | | | | | |
| | IR | RAMAN | Unscaled | Scaled | Relative | Absolute | Relative | Absolute | |
| 60 | | 3580 | 3592 | 3448 | 41 | 9 | 110 | 67 | υ OH(100) |
| 59 | | | 3125 | 3000 | 11 | 2 | 94 | 58 | υ CH(93) |
| 58 | | | 3109 | 2985 | 18 | 4 | 111 | 68 | υ CH(92) |
| 57 | | 2980 | 3087 | 2963 | 38 | 8 | 163 | 100 | υ CH(95) |
| 56 | | | 3075 | 2952 | 1 | 0 | 34 | 21 | υ CH(96) |
| 55 | | | 3060 | 2938 | 24 | 5 | 118 | 72 | υ CH(91) |
| 54 | | | 3054 | 2931 | 39 | 9 | 97 | 59 | υ CH(93) |
| 53 | | | 3020 | 2899 | 40 | 9 | 95 | 58 | υ CH(87) |
| 52 | 2901 | 2888 | 3013 | 2893 | 27 | 6 | 63 | 39 | υ CH(93) |
| 51 | 1643 | 1616 | 1714 | 1647 | 452 | 100 | 6 | 4 | υ ON(95) |
| 50 | | | 1523 | 1463 | 5 | 1 | 5 | 3 | ß HCH(80) |
| 49 | 1428 | 1457 | 1506 | 1447 | 4 | 1 | 6 | 4 | ß HCH(77) |
| 48 | | 1370 | 1424 | 1369 | 3 | 1 | 2 | 1 | ß HOC(19) +ß HCO(18) + |

| | | | | | | | | | |
|---|---|---|---|---|---|---|---|---|---|
| | | | | | | | | | ω CCCH(17) |
| 47 | 1366 | | 1412 | 1357 | 5 | 1 | 3 | 2 | ß HCO(48) + τ HCOC(17) |
| 46 | 1341 | | 1384 | 1330 | 2 | 0 | 5 | 3 | ß HCO(27) + τ HCOC(14) |
| 45 | | | 1363 | 1310 | 14 | 3 | 3 | 2 | ß HCO(25) + τ HCOC(11) |
| 44 | | | 1351 | 1298 | 1 | 0 | 1 | 0 | ß HCO(32) + τ HCOC(10) |
| 43 | 1284 | | 1339 | 1286 | 65 | 14 | 3 | 2 | ß HCO13 + ω CCCH(11) |
| 42 | | | 1324 | 1272 | 34 | 8 | 6 | 4 | ß HCO(44) + τ HCOC(11) + ω CCCH(12) |
| 41 | | 1261 | 1316 | 1265 | 69 | 15 | 3 | 2 | υ ON13 + ß HCO(25) + τ HCON(13) |
| 40 | | | 1309 | 1257 | 128 | 28 | 7 | 4 | υ ON(25) + ß HCO12 + τHCON( 23) |
| 39 | | | 1280 | 1230 | 18 | 4 | 3 | 2 | ß HOC(10) +τ HCOC(18) |
| 38 | | 1211 | 1273 | 1223 | 13 | 3 | 7 | 4 | ß HCO12 + τ HCOC(51) |
| 37 | | | 1231 | 1183 | 2 | 0 | 3 | 2 | ß HCO(72) |
| 36 | | | 1216 | 1169 | 8 | 2 | 2 | 1 | ß HCO(40) |
| 35 | | 1120 | 1212 | 1165 | 41 | 9 | 5 | 3 | ß HOC16 + ß CCO16 + ω OCCC(10) |
| 34 | 1091 | 1091 | 1134 | 1089 | 72 | 16 | 1 | 1 | υ OC(23) |
| 33 | | | 1124 | 1080 | 1 | 0 | 3 | 2 | υ OC(25) |
| 32 | | | 1104 | 1061 | 54 | 12 | 2 | 1 | υ OC(28) + ß HCO(10) |
| 31 | | 1057 | 1094 | 1051 | 19 | 4 | 2 | 1 | υ OC(49) |
| 30 | 1036 | | 1064 | 1023 | 86 | 19 | 5 | 3 | υ OC(41) |
| 29 | | | 1053 | 1012 | 32 | 7 | 3 | 2 | υ CC(21) |
| 28 | | | 1023 | 983 | 127 | 28 | 3 | 2 | υ OC(12) + τ HCON(10) |
| 27 | | | 972 | 934 | 45 | 10 | 4 | 3 | υ OC(21) + τ HCOC(18) |
| 26 | | 948 | 956 | 919 | 21 | 5 | 0 | 0 | υ CC(12 )+ υ OC(28) + ß COC(14) |
| 25 | 899 | | 939 | 902 | 18 | 4 | 4 | 3 | υ CC(26) + υ OC13 |
| 24 | 874 | 876 | 889 | 854 | 29 | 6 | 2 | 1 | υ OC13 + τ HCOC15 |
| 23 | | 850 | 878 | 844 | 14 | 3 | 2 | 1 | υ CC(17) + υ OC(11) |
| 22 | | | 863 | 829 | 181 | 40 | 33 | 20 | υ ON(20) + ß ONO(43) |
| 21 | | | 855 | 821 | 11 | 2 | 12 | 7 | υ OC(27) + υ CC(10) |
| 20 | | 816 | 847 | 814 | 117 | 26 | 2 | 1 | υ OC(13) + ß ONO(16) |
| 19 | 773 | 748 | 775 | 745 | 7 | 2 | 1 | 0 | ß COC(21) + ω OCCC(10) |
| 18 | | | 764 | 734 | 13 | 3 | 1 | 0 | ω OOON(95) |
| 17 | | | 737 | 708 | 65 | 14 | 3 | 2 | ß ONO(16) + ß CCC(11) + ß NOC(16) |
| 16 | | 687 | 685 | 659 | 12 | 3 | 10 | 6 | υ ON(32) + ß ONO(27) + ß OCC(10) + ω OCC(10) |
| 15 | 607 | 591 | 613 | 589 | 8 | 2 | 1 | 1 | ß OCC(12) |
| 14 | | 506 | 593 | 570 | 9 | 2 | 1 | 1 | υ ON10 + ß ONO(26) + ß OCC(12) |
| 13 | | 439 | 465 | 447 | 4 | 1 | 1 | 0 | τ HCOC(11) + τ COCC(11) |
| 12 | | 378 | 402 | 387 | 7 | 2 | 3 | 2 | υ OC(13) + ß OCC(27) |
| 11 | | 354 | 368 | 354 | 3 | 1 | 1 | 0 | ß OCC(39) |
| 10 | | | 338 | 324 | 5 | 1 | 4 | 2 | ß OCC(35) |
| 9 | | | 282 | 271 | 129 | 29 | 2 | 1 | τ HOCC(77) |
| 8 | | 248 | 259 | 249 | 12 | 3 | 2 | 1 | ß OCC(10_ + ß NOC(20) + τ HOCC(18) |
| 7 | | | 213 | 205 | 3 | 1 | 2 | 1 | ß NOC(16) + τ COCC(19) |
| 6 | | 190 | 172 | 165 | 5 | 1 | 0 | 0 | ß OCC(11) + ß NOC(13) + τ HCOC(10) |
| 5 | | | 134 | 129 | 1 | 0 | 0 | 0 | τ CCOC(20) +τ CCCO(24)+ τ COCC(15) |
| 4 | | | 95 | 92 | 3 | 1 | 0 | 0 | τ CCCO(14)+ τ COCC(11) + ωOCCC(23) |
| 3 | | 72 | 86 | 83 | 1 | 0 | 1 | 1 | τ ONOC(30) +τ NOCC(23) |
| 2 | | | 58 | 56 | 1 | 0 | 1 | 1 | τ ONOC(44) +τ NOCC(18) |
| 1 | | | 44 | 42 | 0 | 0 | 0 | 0 | τ CCCO(19)+ τ NOCC(48) |

Abbreviations: υ-stretching vibration; ß-in plane bending; ω-out of plane bending; τ-torsion

### *4.2.1 O-H Vibrations*

The presence of an O-H group leads to three modes of vibration, viz. stretching, in-plane bending and out of the plane bending vibrations. O-H stretching vibrations are are characterized by broad bands in the region 3600-3400$cm^{-1}$[20]. These vibrations are more sensitive towards hydrogen bonding [21]. The presence of hydrogen bond alters the frequencies of stretching and bending vibrations. These bands move to a lower frequency with greater intensity and band broadens in the hydrogen bonded species. The presence of hydrogen bonding in five or six member ring system would decline the O–H stretching band to 3550-3200 $cm^{-1}$ region [22]. In the present study, the peak corresponding to 3448$cm^{-1}$ is in the DFT method is due to the O-H vibration. The peak at 3580$cm^{-1}$ of the Raman band also corresponds to the O-H stretching vibration. The PED contribution of O-H stretching is found to be 100%, which suggest that it is a pure stretching mode.

*4.2.2 C-H Vibrations*

The characteristic wavenumber region for C-H stretching in the aromatic compounds is 3100-3000 $cm^{-1}$[23]. These are not affected by the type of the substituent to a great extend [24,25]. In the current study, we have 6 peaks that correspond to the C-H Stretching vibration in B3LYP/6-311++G(d,p). They are 3013, 2997, 2976, 2965, 2950, 2944, 2912 $cm^{-1}$. The peak at 2980$cm^{-1}$ in Raman band corresponds to C-H stretching. The PED contribution ranges from 87-96%.

4.2.3 *NO Vibrations*

One of the most characteristic bands in the spectrum of nitro compounds owed to $NO_2$ stretching vibration. It is very useful not only due to the spectral position but also because of the strong intensity as well [26]. The asymmetric $NO_2$ stretching vibrations are found in the region 1580±80 $cm^{-1}$, whereas the symmetric $NO_2$ stretching vibrations are expected to be in the region 1380±20$cm^{-1}$. In this case the strong band observed at 1643$cm^{-1}$ in FT-IR, 1616 in FT-Raman and 1652 $cm^{-1}$ in B3LYP/6-311++G(d,p) corresponds to NO stretching vibration with a PED contribution of 95%. Modes numbered 41(13), 40(25%), 22(20%), 16(32%), 14(10%) have notable PED contribution. Peaks at 832, 816, 710, 661, 572 $cm^{-1}$ in theoretical wavenumber corresponds to in plane bending $NO_2$ with PED ranging from 43% to 16% and is found that to be in agreement with the experimental values.

*4.3 Non-Linear optical effects*

One of the major areas of today's research is on Non linear Optics as it provides the vital functions for emerging technologies in the areas of telecommunication, signal processing and interconnections, which include frequency shifting, optical modulation, optical switching, optical logic and optical memory [27,28]. The dipole moment, polarizability and first order hyperpolarizability for Isosorbide mononitrate have been calculated using the basis set B3LYP/6-311++G(d,p) and are listed in the table 3. The first order hyperpolarizability of the title compound was found to be $1.95x10^{-31}$e.s.u which is greater than that of the first order hyperpolarizability of

Urea(0.372 x$10^{-31}$e.s.u) which is the prototypical molecule used to evaluate the NLO properties of a compound [29].

Table 3: The calculated values of dipole moment **μ** (D), polarizability ($\boldsymbol{\alpha_0}$), first order hyperpolarizability ($\boldsymbol{\beta_{tot}}$) components of Isosorbide Mononitrate.

| PARAMETER | B3LYP/6-311++G(d,p) | PARAMETER | B3LYP/6-311++G(d,p) |
|---|---|---|---|
| $\mu_x$ | 0.216 | $\beta_{xxx}$ | -46.916 |
| $\mu_y$ | -0.771 | $\beta_{xxy}$ | 16.078 |
| $\mu_z$ | 1.182 | $\beta_{xyy}$ | -46.446 |
| **μ(D)** | 1.427 | $\beta_{yyy}$ | -70.306 |
| $\alpha_{xx}$ | 79.340 | $\beta_{zxx}$ | -36.127 |
| $\alpha_{xy}$ | 1.649 | $\beta_{xyz}$ | 52.256 |
| $\alpha_{yy}$ | 85.780 | $\beta_{zyy}$ | -14.286 |
| $\alpha_{xz}$ | 21.076 | $\beta_{xzz}$ | -100.687 |
| $\alpha_{yz}$ | -15.019 | $\beta_{yzz}$ | 76.658 |
| $\alpha_{zz}$ | 110.872 | $\beta_{zzz}$ | -62.372 |
| α (a.u) | 91.997 | $\beta_{tot}$ (a.u) | 225.563 |
| α (e.s.u) | 1.36x$10^{-23}$ | **$\beta_{tot}$ (e.s.u)** | 1.95x$10^{-30}$ |
| Δα (a.u) | 140.418 | | |
| **$\Delta\alpha_0$ (e.s.u)** | 2.08x$10^{-23}$ | | |

### *4.4 Frontier Molecular Orbital Analysis*

One of the vital tools quantum chemistry offers is the study of the HOMO (highest occupied molecular orbital) and LUMO (lowest unoccupied molecular orbital). HOMO can be regarded as the outer most orbital which contain electrons and tends to give these electrons away (electron donor), whereas LUMO can be considered as the inner most orbital containing free places to accept electrons [30]. The graphical representation of HOMO and LUMO is shown in Fig 4. The HOMO energy for the title compound was found to be -7.627eV and LUMO energy -2.41eV. The energy gap (energy difference between the HOMO and LUMO orbitals) was found to be 5.215eV. It serves as an important stability factor for the compound [31]. The energy gap for the title compound confirms that the molecule has stable structure. Lower the energy gap, easier the electrons are excited from the ground state to excited state.
Properties like Chemical potential (μ), Electro negativity (χ), Global hardness (η), Electrophilicity, Softness (S) can be calculated using the following relations based on the energy value of HOMO and LUMO [32]. These have been listed in table 4.

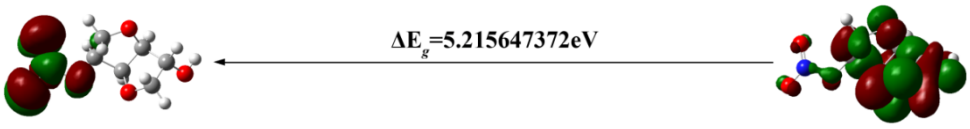


Fig 4: Plot for HOMO-LUMO of Isosorbide Mononitrate.

Table 4: Calculated energy values of title compound using B3LYP/6-311++G(d,p) method.

| PROPERTY | B3LYP/6-311++G(d,p) |
|---|---|
| HOMO(eV) | -7.627 |
| LUMO(eV) | -2.412 |
| Ionization potential | 7.627 |
| Electron affinity | 2.412 |
| Energy gap(eV) | 5.216 |
| Electronegativity | 5.020 |
| Chemical potential | -5.020 |
| Chemical hardness | 2.608 |
| Chemical softness | 0.192 |
| Electrophilicity index | 4.831 |

*Chemical potential ($\mu$) = $\frac{1}{2}(E_{LUMO} + E_{HOMO})$

*Electro negativity ($\chi$) = $-\mu = -\frac{1}{2}(E_{LUMO} + E_{HOMO})$

*Global hardness ($\eta$) = $\frac{1}{2}(E_{LUMO} - E_{HOMO})$

*Electrophilicity = $\frac{\mu}{2\eta}$

*Softness (S) = $\frac{1}{\eta}$

*[33-35]

Energy of 7.67eV is necessary to remove an electron from HOMO which is indicated by the ionization potential. Lesser the value of electron affinity shows higher molecular reactivity with the nucleophiles. Higher hardness and lower softness values prove the higher molecular hardness associated with the molecule. The electrophilicity index helps in describing the biological activity of title compound[36-38].

### *4.5 Molecular Electrostatic Potential (MEP)*

Complete mapping of the title compound was carried out based on the electrostatic potential on the surface. MEP diagram gives the three dimensional visualization of the charge distributions and the charge related properties of the molecule. With the help of the MEP diagram we can easily predict the possible sites of electrophillic and

nucleophillic attack on the compound and are useful in hydrogen bond interaction as well as in biological recognition process [39]. Electrostatic potential of the region on the surface of the compound is differentiated by means of colour coding. Red indicates region with most electronegative electrostatic potential; blue represents region with most electropositive electrostatic potential; and green denotes the area with zero potential. The electrostatic potential scales in the order of red < orange < yellow < green < blue[40]. MEP diagram for the title compound using DFT is given in Fig 5. The colour code of this map ranges from -6.388eV to 6.388eV. From the Fig 5 we can find that the red regions (negative) are localized near the O and N atoms which are the most probable site for electrophillic attack. The Blue region (positive) is found to be near the H atoms which are the most probable site for nucleophillic attack. The contour map of electrostatic potential validates the different negative and positive potential sites of the molecule in accordance with the total electron density surface map.

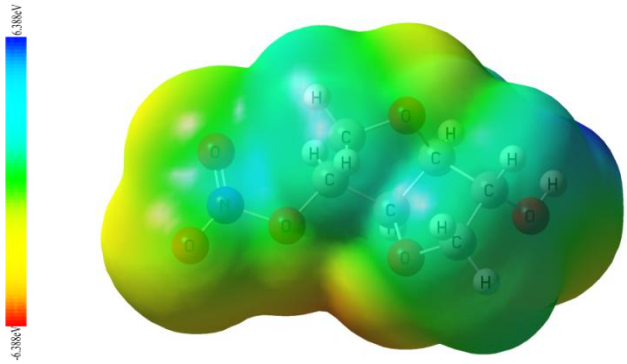


Fig 5: Molecular Electrostatic Potential of the title compound.

*4.6 Thermodynamic properties*

The standard thermodynamic properties {heat capacity ($C_p$), entropy (S) and enthalpy changes (H)} for the title compound was determined using the Perl script THERMO.PL and are listed in table 5. The correlation equations between temperatures and heat capacity, entropy, enthalpy changes were fitted by quadratic formulae and the corresponding fitting factor ($R^2$) were calculated and are shown below.

$C = 24.55451 + 0.61164T - 1.98633 \times 10^{-4} T^2 (R^2 = 0.998)$

$S = 242.6446 + 0.75975T - 1.9403 \times 10^{-4} T^2 (R^2 = 0.99984)$

$H = -1.15135 + 0.04486T + 2.35094 \times 10^{-4} T^2 (R^2 = 0.9999)$

The above equation can be used to study the title compound further. The Gibbs free energy of reaction that will help to find the spontaneity of the reaction can be studied [41].

Table 5: Deviation of thermodynamic property with temperature.

| T(K) | $S_m^0$(J/mol.K) | $C_{p,m}$(J/mol.K) | $H_m^0$(kJ/mol) |
|---|---|---|---|
| 100 | 314.699 | 88.614 | 6.062 |
| 200 | 389.764 | 133.355 | 17.144 |

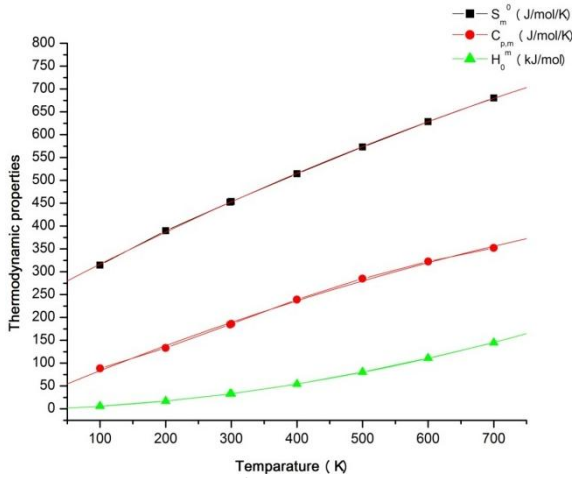


Fig 6: Correlation graph for thermodynamic properties (Entropy, Heat capacity, Enthalpy) vs. Temperature.

| | | | |
|---|---|---|---|
| 298.15 | 452.346 | 184.752 | 32.696 |
| 300 | 453.492 | 185.77 | 33.039 |
| 400 | 514.371 | 239.239 | 54.329 |
| 500 | 572.865 | 285.232 | 80.628 |
| 600 | 628.274 | 322.315 | 111.075 |
| 700 | 680.27 | 351.978 | 144.844 |

### *4.6 Fukui function*

Fukui function is accepted as the local density functional descriptors to depict chemical reactivity and selectivity. Fukui function is introduced to predict electrophillic and nucleophillic reactions within a molecule. Fukui functions can be calculated using the following equations:

$f_k^- = q_{k(N)} - q_{k(N-1)}$ for electrophilic attack

$f_k^+ = q_r(N+1) - q_k(N)$ for nucleophilic attack

$f_k^0 = 1/2\,[q_k(N+1) - q_k(N-1)]$ for radical attack

In these equations, $q_k$ is the charge at the kth atomic site is the neutral (N), anionic (N+1), cationic (N-1) chemical species [42-45].

The local softness is related to Fukui function as follows:

$s_k - f_k - = Sf^-_k$ for electrophilic attack

$s_k + f_k + = Sf^+_k$ for nucleophilic attack

$s_k 0\ f_k 0 = Sf^0_k$ for radical attack

The regions of a molecule where the Fukui function is large are chemically softer than the regions where the Fukui function is small. Fukui functions and local softness for selected atomic sites in the title compound are listed in Table 6. It has been found that for the title compound the possible sites for nucleophillic attack is O2,C3,C4,O9. The radical attack was predicted at C3,C4,C8.

Table 6: Fukui function $f_k$ and descriptors $(sf)_k$

| **Atoms** | $f_k^+$ | $f_k^-$ | $f_k^0$ | $(sf)_k^+$ | $(sf)_k^-$ | $(sf)_k^0$ |
|---|---|---|---|---|---|---|
| C1 | -0.38378 | 0.035404 | -0.17419 | -0.08025 | 0.007403 | -0.03642 |
| O2 | 0.047566 | -0.14238 | -0.04741 | 0.009946 | -0.02977 | -0.00991 |
| C3 | 0.393086 | 0.037917 | 0.215502 | 0.082194 | 0.007928 | 0.045061 |
| C4 | 0.475569 | 0.028801 | 0.252185 | 0.099441 | 0.006022 | 0.052732 |

| | | | | | | |
|---|---|---|---|---|---|---|
| C5 | -0.01584 | 0.006364 | -0.00474 | -0.00331 | 0.001331 | -0.00099 |
| O6 | -0.0181 | -0.13446 | -0.07628 | -0.00379 | -0.02812 | -0.01595 |
| C7 | -0.07466 | 0.055548 | -0.00956 | -0.01561 | 0.011615 | -0.002 |
| C8 | 0.328943 | 0.049427 | 0.189185 | 0.068782 | 0.010335 | 0.039559 |
| O9 | -0.04519 | -0.07068 | -0.05794 | -0.00945 | -0.01478 | -0.01211 |
| O10 | -0.10969 | -0.02005 | -0.06487 | -0.02294 | -0.00419 | -0.01356 |
| N11 | -0.29941 | -0.01918 | -0.15929 | -0.06261 | -0.00401 | -0.03331 |
| O12 | -0.05515 | -0.0437 | -0.04943 | -0.01153 | -0.00914 | -0.01034 |
| O13 | -0.09636 | -0.0977 | -0.09703 | -0.02015 | -0.02043 | -0.02029 |
| H14 | -0.24755 | -0.09733 | -0.17244 | -0.05176 | -0.02035 | -0.03606 |
| H15 | -0.02192 | -0.10285 | -0.06238 | -0.00458 | -0.02151 | -0.01304 |
| H16 | -0.24165 | -0.07058 | -0.15611 | -0.05053 | -0.01476 | -0.03264 |
| H17 | -0.06094 | -0.06822 | -0.06458 | -0.01274 | -0.01426 | -0.0135 |
| H18 | -0.04679 | -0.08468 | -0.06574 | -0.00978 | -0.01771 | -0.01375 |
| H19 | -0.06513 | -0.11342 | -0.08927 | -0.01362 | -0.02372 | -0.01867 |
| H20 | -0.05365 | -0.0597 | -0.05667 | -0.01122 | -0.01248 | -0.01185 |
| H21 | -0.1525 | -0.06291 | -0.10771 | -0.03189 | -0.01315 | -0.02252 |
| H22 | -0.25687 | -0.02563 | -0.14125 | -0.05371 | -0.00536 | -0.02953 |

*4.7 NBO Analysis*

Natural bond orbital analysis helps to investigate the charge transfer or conjugative interaction in molecular systems. NBO analysis was performed on the title compound at B3LYP/6-311++G(d,p) level in order to explain the intramolecular, rehybridizaion and delocalization of electron density within the molecule [46]. From the second order perturbation approach the hyper conjugative interaction energy was deduced. For each donor NBO (i) and acceptor NBO (j) the stabilization energy $E^{(2)}$ related with electron delocalization between donor and acceptor is estimated as

$$E^{(2)} = \Delta E_{ij} = \frac{q_i(F_{ij})^2}{\varepsilon_j - \varepsilon_i}$$

where $\mathbf{q_i}$ is the donor orbital occupancy $\boldsymbol{\varepsilon_j}$ and $\boldsymbol{\varepsilon_i}$ are diagonal elements, $\mathbf{F_{ij}}$ is the off diagonal NBO Fock matrix element [47]. The larger the $E^{(2)}$ value the more intensive is the interaction between electron donors and greater the extend of conjugation of the whole system.

The hyperconjugative interaction of σ to $\sigma^*$ transition occur from various bonds in the title compound. The σ (C1-C8) to their antibonding $\sigma^*$ (O10-N11) leads to a stabilization energy of 5.73 kcal/mol. The most interaction energy, related to the resonance in the molecule is the electron donating from LP(3) O13 to the antibonding $\sigma^*$(N11-O12) which leads to a stabilization energy of 96.41kcal/mol as shown in Table 7.

Table 7: Second order perturbation theory analysis of Fock matrix in selected NBO basis calculated at B3LYP/6-311++G(d,p)

| DONOR | TYPE | ED/e | ACCEPTOR | TYPE | ED/e | E(2)[a] (kcal/mol) | E(j)-E(i)[b] a.u | F(i,j)[c] a.u |
|---|---|---|---|---|---|---|---|---|
| C1 - C8 | σ | 1.94911 | O10 - N11 | σ* | 0.36274 | 5.73 | 0.58 | 0.056 |
| C1 - H14 | σ | 1.98025 | C5 - O6 | σ* | 0.02676 | 2.51 | 0.84 | 0.041 |
| C3 - H15 | σ | 1.98538 | C4 - O9 | σ* | 0.01985 | 2.11 | 0.8 | 0.037 |
| C3 - H16 | σ | 1.98483 | C1 - O2 | σ* | 0.02803 | 2.63 | 0.82 | 0.042 |
| C3 - H16 | σ | 1.98483 | C4 - C5 | σ* | 0.02894 | 1.25 | 0.9 | 0.03 |
| C4 - C5 | σ | 1.96553 | C1 - O2 | σ* | 0.02803 | 1.96 | 0.94 | 0.038 |
| C4 - C5 | σ | 1.96553 | O6 - C7 | σ* | 0.01746 | 2.23 | 0.95 | 0.041 |
| C4 - H17 | σ | 1.97765 | C3 - H15 | σ* | 0.03071 | 1.97 | 0.87 | 0.037 |
| C4 - H17 | σ | 1.97765 | C5 - O6 | σ* | 0.02676 | 2.23 | 0.82 | 0.038 |
| C5 - H18 | σ | 1.97762 | C1 - O2 | σ* | 0.02803 | 2.5 | 0.83 | 0.041 |
| C7 - C 8 | σ | 1.98163 | C1 - H14 | σ* | 0.03547 | 2.24 | 1.01 | 0.043 |
| C7 - H19 | σ | 1.98572 | C8 - O10 | σ* | 0.03366 | 2.2 | 0.8 | 0.038 |
| C7 - H20 | σ | 1.98182 | C5 - O6 | σ* | 0.02676 | 2.79 | 0.83 | 0.043 |
| C7 - H 20 | σ | 1.98182 | C8 - O10 | σ* | 0.03366 | 2.45 | 0.8 | 0.04 |
| C8 - H21 | σ | 1.97559 | C1 - O2 | σ* | 0.02803 | 1.91 | 0.84 | 0.036 |
| O9 - H22 | σ | 1.98848 | C4 - C5 | σ* | 0.02894 | 1.94 | 1.13 | 0.042 |
| O10 - N11 | σ | 1.97181 | O10 - N11 | σ* | 0.36274 | 2.19 | 0.65 | 0.037 |
| O10 - N11 | σ | 1.97181 | N11 - O13 | σ* | 0.06804 | 4.21 | 0.96 | 0.057 |
| N11 - O12 | σ | 1.99765 | N11 - O12 | σ* | 0.03298 | 3.61 | 0.41 | 0.04 |
| O 2 | LP (1) | 1.96748 | C3 - H16 | σ* | 0.01667 | 2.1 | 0.95 | 0.04 |
| O 2 | LP (2) | 1.91476 | C1 - C5 | σ* | 0.04146 | 3.14 | 0.68 | 0.042 |
| O 2 | LP (2) | 1.91476 | C1 - H14 | σ* | 0.03547 | 7.44 | 0.67 | 0.064 |
| O 2 | LP (2) | 1.91476 | C3 - C4 | σ* | 0.0323 | 3.19 | 0.7 | 0.043 |
| O 2 | LP (2) | 1.91476 | C3 - H15 | σ* | 0.03071 | 7.45 | 0.66 | 0.064 |
| O 6 | LP (2) | 1.90823 | C1 - C5 | σ* | 0.04146 | 2.67 | 0.68 | 0.039 |
| O 6 | LP (2) | 1.90823 | C5 - H18 | σ* | 0.04167 | 10.15 | 0.67 | 0.075 |
| O 6 | LP (2) | 1.90823 | C7 - C8 | σ* | 0.03604 | 2.42 | 0.68 | 0.037 |
| O 6 | LP (2) | 1.90823 | C7 - H19 | σ* | 0.02825 | 7.9 | 0.67 | 0.066 |
| O 9 | LP (2) | 1.90823 | C3 - C4 | σ* | 0.0323 | 2.99 | 0.74 | 0.042 |

| | | | | | | | | |
|---|---|---|---|---|---|---|---|---|
| O 9 | LP (2) | 1.90823 | C4 - H17 | σ* | 0.0366 | 9.3 | 0.7 | 0.072 |
| O 10 | LP (1) | 1.97867 | N11 - O12 | π* | 0.03298 | 2.97 | 1.29 | 0.055 |
| O 10 | LP (2) | 1.88071 | C7 - C8 | σ* | 0.03604 | 5.24 | 0.71 | 0.056 |
| O 10 | LP (2) | 1.88071 | C7 - H19 | σ* | 0.02825 | 0.62 | 0.7 | 0.019 |
| O 10 | LP (2) | 1.88071 | C 8 - H21 | σ* | 0.03223 | 6.72 | 0.69 | 0.062 |
| O 10 | LP (2) | 1.88071 | N11 - O12 | σ* | 0.52254 | 14.51 | 0.21 | 0.055 |
| O 12 | LP (1) | 1.97665 | N11 - O13 | σ* | 0.06804 | 3.69 | 1.08 | 0.057 |
| O 12 | LP (2) | 1.74897 | O10 - N11 | σ* | 0.36274 | 65.18 | 0.28 | 0.125 |
| O 12 | LP (2) | 1.74897 | N11 - O13 | σ* | 0.06804 | 19.96 | 0.6 | 0.103 |
| O 13 | LP (1) | 1.9839 | N11 - O12 | π* | 0.03298 | 3.94 | 1.42 | 0.067 |
| O 13 | LP (2) | 1.84759 | O10 - N11 | σ* | 0.36274 | 32.48 | 0.27 | 0.089 |
| O 13 | LP (2) | 1.84759 | N11 - O12 | π* | 0.03298 | 6.53 | 0.93 | 0.072 |
| O 13 | LP (2) | 1.84759 | N11 - O13 | σ* | 0.06804 | 2.52 | 0.59 | 0.035 |
| O 13 | LP (3) | 1.5527 | N11 - O12 | σ* | 0.52254 | 96.41 | 0.16 | 0.114 |
| O10 - N11 | σ* | 0.36274 | C8 - O10 | σ* | 0.03366 | 3.23 | 0.35 | 0.068 |
| O10 - N11 | σ* | 0.36274 | N11 - O13 | σ* | 0.06804 | 3.01 | 0.32 | 0.06 |

[a] E(2) is the energy of the hyper conjugative interaction(stabilization energy).
[b]Energy difference between donor and acceptor i and j NBO orbitals.
[c]F(i,j) is the Fock matrix element between i and j NBO orbitals.

### *4.8 Mulliken Population Analysis*

The charge distribution of the title compound was analyzed using Mulliken method with B3LYP/6-311++G(d,p) level theory. It depicts charge of each atom in the molecule. Distribution of positive and negative charges also has an effect on the bond length [48]. From Fig it can be seen that hydrogen atoms are positively charged whereas the magnitude of atomic charges on oxygen atom were calculated to be both positive and negative. Nitrogen atoms have large negative charge and behave as electron donor (Fig 7).

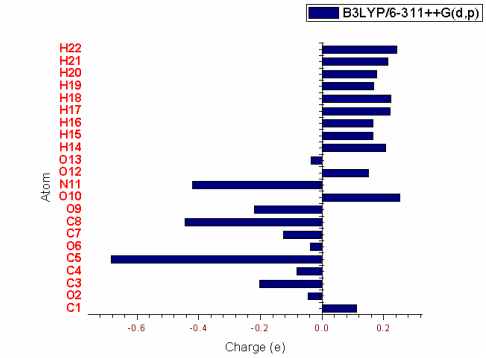


Fig 7: Mulliken charge distribution for atoms of Isosorbide mononitrate using B3LYP/6-311++ G(d,p)

## 5. Conclusion

Spectroscopic (FT-IR, FT-Raman,), NLO, NBO, MEP and thermodynamic function of Isosorbide mononitrate was analyzed using B3LYP/6-311++G(d,p) basis set. The complete vibrational assignments and the calculation of Potential Energy Distribution (PED) were carried out using the VEDA 4 software. The experimental results are in conformity with the theoretical values derived from structural parameters, vibrational frequencies, infrared intensities and Raman activities. The Non-Linear Optical (NLO) properties were calculated theoretically and it was found that the predicated first hyperpolarizability value is greater than that of Urea. This points to the fact the title compound show good NLO effects. The HOMO and LUMO energies were calculated and the energy gap was determined as 5.215eV. The electrophilicity values were calculated from the HOMO and LUMO energies and found to be significantly high. This confirms that the title compound is biologically active. The predicted MEP diagram gives out the negative and positive regions of the molecule. NBO analysis was done on the title compound and it showed that the intra molecular charge transfer occurs between the bonding and antibonding orbitals. The thermodynamic properties of the title compound were calculated for different temperatures, and the correlations among the properties and temperatures were obtained. This data in turn will prove to be useful for further study on the title compound with relation to thermodynamic properties. The charge distribution was also found out using the Mulliken population analysis.

## 6. REFERENCES

[1] Moncada, S. Palmer, P.M. Higgs, E.A. Nitric oxide: physiology, pathophysiology, and pharmacology. *Pharmacol Rev*, 43,2,( 1991),109-42.

[2] Mancuso, C. Navarra, P. Preziosi, P. Roles of nitric oxide, carbon monoxide, and hydrogen sulfide in the regulation of the hypothalamic-pituitary-adrenal axis. *J Neurochem* 113, 3, (2010), pp.563-575.
[3] Ekerhovd,E. Bullarbo,M. Andersch, B. Vaginal administration of the nitric oxide donor isosorbide mononitrate for cervical ripening at term: a randomized controlled study, *American J. Cardiology (2003)*.
[4] Bogaert, M.G. and Rosseel, M.T. Naunyn, Vascular effects of the dinitrate and mononitrate esters of isosorbide, isomannide and isoidide *Schmiedeberg's Arch. Pharmacol*. 275, 3, (1972), pp. 339–342.
[5] Bharani, A. Ganguli, A. Mathur ,L.K. Jamra ,Y. Raman,P.G. Efficacy of Terminalia arjuna in chronic stable angina: a double-blind, placebo-controlled, crossover study comparing Terminalia arjuna with isosorbide mononitrate. *Indian Heart Journal*, 54, 2, (2002), pp. 170-175.
[6] Steven Chrysant, G. Glasser, P. Neville Bittar, Eden Shahidi, Kola Danisa, Ibrahim, Earl Watts, Ronald Garutti, J. Rudolfo Ferraresi, Roberto Casareto, Efficacy and safety of extended-release Isosorbide Mononitrate for stable effort angina pectoris, *The American Journal of Cardiology*, 72, 17, (1993), pp. 1249-1256.
[7] Càndid Villanueva. Joaquim Balanzó. Maria Novella, German Soriano, T. Sergio Sáinz. Xavier Torras. Xavier Cussó. Carlos Guarner. Francisco Vilardell. Nadolol plus Isosorbide Mononitrate Compared with Sclerotherapy for the Prevention of Variceal Rebleeding, N Engl. *J Med*, 334,( 1996) p.p 1624-1629
[8] Frisch, M.J. Trucks, G. W. Schlegel, H. B. Scuseria, G. E. Robb, M. A. Cheeseman, J. R. Scalmani, G. Barone, V. Mennucci, B. Petersson, G. A. Nakatsuji, H. Caricato, M. Li, X. Hratchian, H. P. Izmaylov, A. F. Bloino, J. G. Zheng, J. L. Sonnenberg, M. Hada, M. Ehara, K. Toyota, R. Fukuda, J. Hasegawa, Ishida, M. Nakajima, T. Honda, Y. Kitao, O. Nakai, H. Vreven, T. Montgomery, J. A. Jr., Peralta, J. E. Ogliaro, F. Bearpark, M. Heyd, J. J. Brothers, E. Kudin, K. N. Staroverov, V. N. Kobayashi, R. Normand, J. Raghavachari, K. Rendell, A. Burant, J. C. Iyengar, S. S. Tomasi, J. Cossi, M. Rega, N. Millam, J. M. Klene, M. Knox, J. E. Cross, J. B. Bakken, V. Adamo, C. Jaramillo, J. Gomperts, R. Stratmann, R. E. Yazyev, O. Austin, A. J. Cammi, R. Pomelli, C. Ochterski, J. W. Martin, R. L. Morokuma, K. Zakrzewski, V. G. Voth, G. A. Salvador, P. Dannenberg, J. J. Dapprich, S. Daniels, A. D. Farkas, Ö. Foresman, J. B. Ortiz, J. V. Cioslowski, J. and Fox D. J., Gaussian 09 (Gaussian, Inc., Wallingford CT, 2009).
[9] Sundaraganesan, Illakiamani N. Saleem, H. Wojciechowski, P.M. Michaliska, D. FT Raman and FT-IR spectra, vibrational assignments and density functional studies of 5-bromo-2-nitropyridine, *Spectrochim. Acta 61A*, (2005), pp. 2995-3001.
[10] Jamroz, H. Vibrational Energy Distribution Analysis VEDA 4, Warsaw, 2004
[11] Sylaja, B. Srinivasan, S. Ab Initio and Density Functional Theory (DFT) Study on Clonazepam, *Open Journal of Biophysics*, 2, (2012), pp.80-87.

[12] Jamroz, M.H. Dobrowolski, J.C. Brzozowski, R. Vibrational modes of 2,6-, 2,7-, and 2,3-iisopropylnaphthalene. A DFT study, *J. Mol. Struct.*, 787, (2006), pp. 172-183.
[13] Cırak, C. Demir, S. Ucun, F. Cubuk, O. Experimental and theoretical study on the structure and vibrational spectra of β-2-aminopyridinium dihydrogenphosphate, *Spectrochim. Acta Part* A, 79, (2011), pp. 529-532.
[14] Arslan, H. Algul, O. Vibrational spectrum and assignments of 2-(4-methoxyphenyl)-1Hbenzo[d]imidazole by ab initio Hartree-Fock and density functional methods, *Spectrochim. Acta Part* A ,70, (2008), pp.109-116.
[15] GaussView, Version 5, Roy Dennington, Todd Keith, and John Millam, Semichem Inc., Shawnee Mission, K.S, (2009).
[16] Glendenning, E.D. Reed, A.E. Carpenter, J.E. Weinhold, NBO version 3.1,TCL,University of Wisconsin, Madison, (1998).
[17] Oreshko, G.V. Eremenko, L.T. Lagodzinskaya, G.V. Aleksandrov, G.G. Ermenko, I.L. *Russ. Chem. Bull*, 57, (2008) pp. 2185–2189.
[18] Uma Maheswari, J. Muthu, S. Tom Sundius. An experimental and theoretical study of the vibrational spectra and structure of Isosorbide dinitrate, *Spectrochimica Acta Part A: Molecular and Biomolecular Spectroscopy*, 109, (2013) pp.322–330.
[19] Foresman, J.B. Frisch, E. Exploring Chemistry with Electronic Structure Methods, vol. 118, *Gaussian*, Pittsburgh, PA, (1996).
[20] Bhavani, K. Renuga, S. Muthu, S. Sankara narayanan, K. Quantum mechanical study and spectroscopic (FT-IR, FT-Raman, 13C, 1H) study, first order hyperpolarizability, NBO analysis, HOMO and LUMO analysis of 2-acetoxybenzoic acid by density functional methods *Spectrochimica Acta Part A: Molecular and Biomolecular Spectroscopy*, 136, (2015), pp.1260–1268
[21] Choperena, A. Painter, P. An infrared spectroscopic study of hydrogen bonding in ethyl phenol: A model system for polymer phenolics, *Vib. Spectrosc*, 51, (2009), pp.110–118.
[22] Sathyanarayana, D.N. Vibrational Spectroscopy Theory and Applications, second ed., New Age International Publishers, New Delhi, (2004)
[23] Swarnalatha, N. Gunasekaran, S. Muthu, S. Nagarajan, M. Molecular structure analysis and spectroscopic characterization of 9-methoxy-2H-furo[3,2-g]chromen-2-one with experimental (FT-IR and FT-Raman) techniques and quantum chemical calculations,S*pectrochim. Acta* part A, 137, (2015) pp. 721-729.
[24] Dollish, F.R. Fateley, W.G. Bentley, F.F. Characteristic Raman Frequencies of Organic Compounds, *Wiley*, New York, (1997).
[25] Varsanyi, G. Vibrational Spectra of Benzene Derivatives, Academic Press, New York, (1969).
[26] Roeges, N.P.G. A Guide to the Complete Interpretation of Infrared Spectra of Organic Structures, *Wiley*, New York, (1994).
[27] Karabacak, M. Kurt, M. Atac, A. Experimental and theoretical FT-IR and FT-Raman spectroscopic analysis of N1-methyl-2-chloroaniline, *J. Phys. Org. Chem*, 22, 4, (2009), pp. 321–330.

[28] Sajan, D. Joe, H. Jayakumar, V.S. Zaleski, J. Structural and electronic contributions to hyperpolarizability in methyl p-hydroxy benzoate, *J. Mol. Struct*. 785, (2006), pp. 43–53.
[29] Raja, M. Muhamed, R.R. Muthu, S. Suresh, M. Synthesis, spectroscopic (FTIR,FT-Raman, NMR, UV–Visible), first order hyperpolarizability, NBO and molecular docking study of (E)-1-(4-bromobenzylidene)semicarbazide, *Journal of Molecular Structure* (2016),
[30] Muthu, S. Renuga, S. Vibrational spectra and normal coordinate analysis of 2-hydroxy-3-(2-methoxyphenoxy) propyl carbamate, *Spectrachim. Acta* A, 132, (2014) pp. 313–325.
[31] Lewis, D. F. V. loannides, C. Parke, D. V. Interaction of a series of nitriles with the alcohol-inducible isoform of P450: Computer analysis of structure—activity relationships, *Xenobiotica*, 24,5, (1994) pp.401–408.
[32] Parr, R. G. Donnelly, R. A. Levy, M. and Palke, W. E. Electronegativity: the density functional viewpoint, The Journal of Chemical Physics, vol. 68, no. 8, pp. 3801–3807, 1977.
[33] Parr, R. G. and Pearson, R. G. activation hardness: new index for describing the orientation of electrophilic aromatic substitution, *Journal of the American Chemical Society*, 105, 26, (1983), pp. 7512–7516,
[34] Pearson, R. G. Inorganic Chemistry, 27, 4, (1988), pp. 734–740
[35] Geerlings, P. De Proft, F. and Langenaeker, W. "Conceptual density functional theory," *Chemical Reviews*, 103, 5, (2003) pp. 1793–1873.
[36] Parthasarathi, R. Padmanabhan, J. Elango, M. Subramanian, V. Chattaraj, P. Intermolecular reactivity through the generalized philicity concept, *Chem. Phys. Lett*, 394, (2004), pp. 225–230.
[37] Parthasarathi, R. Padmanabhan, J. Subramanian, V. Maiti, B. Chattaraj, P. Toxicity analysis of 33'44'5-pentachloro biphenyl through chemical reactivity and selectivity profiles, *Curr. Sci.*, 86, (2004), pp. 535–542.
[38] Parthasarathi, R. Padmanabhan, J. Subramanian, V. Sarkar, U. Maiti, B. Chattaraj, P. Toxicity analysis of benzidine through chemical reactivity and selectivity profiles: a DFT approach, Internet Electron. *J. Mol. Des.*, 2, (2003), pp. 798–813.
[39] Politzer, P. Murray, J.S. in: D.L. Beveridge, R. Lavery (Eds.) Theoretical Biochemistry and Molecular Biophysics, A comprehensive Survey, protein, Vol. 2, Adenine Press, Schenectady, New York (1991).
[40] Thul, P. Gupta, V.P. Ram, V.J. Tandon, P. Structural and spectroscopic studies on 2-pyranones, *Spectrochim. Acta*, 75, (2010), pp. 251.
[41] Swarnalatha, N. Gunasekaran, S. Muthu, S. Nagarajan, M. Molecular structure analysis and spectroscopic characterization of 9-methoxy-2H-furo[3,2-g]chromen-2-one with experimental (FT-IR and FT-Raman) techniques and quantum chemical calculations *Spectrochimica Acta Part A: Molecular and Biomolecular Spectroscopy*, 137, (2015), pp. 721–729
[42] Kolandaivel, P. Praveen, G. Selvarengan, P. Study of atomic and condensed atomic indices for reactive sites of molecules, *J. Chem. Sci.*, 117, (2005), pp. 591-598.

[43] Muthu, S. Isac Paulraj, E. Spectroscopic and molecular structure (monomeric and dimeric structure) investigation of 2-[(2-hydroxyphenyl) carbonyloxy] benzoic acid by DFT method: a combined experimental and theoretical study, *J. Mol. Struct*., 1038, (2013), pp. 145-162.

[44] Weitao Yang, Wilfried Mortier, J. The use of global and local molecular parameters for the analysis of the gas-phase basicity of amines, *J. Am. Chem. Soc.*, 108, (1986), pp. 5708-5711.

[45] Sun, Y.X. Hao, Q.L. Wei, W.X. Yu, Z.X. Lu, L.D. Wang, X. Wang, Y.S. Experimental and density functional studies on 4-(3, 4-dihydroxybenzylideneamino) antipyrine, and 4-(2, 3, 4-trihydroxybenzylideneamino) antipyrine, *J. Mol. Struct. THEOCHEM*, 904, (2009), pp. 74-82.

[46] Snehalatha, M. Ravikumar, C. Hubert Joe, I. Sekar, N. Jayakumar, V.S. Spectroscopic analysis and DFT calculations of a food additive Carmoisine, *Spectrochim. Acta 72*A, 654 (2009).

[47] Sidir, I. Sidir, Y.G. Kumalar, M. Tasal, E. Ab initio Hartree-Fock and density functional theory investigations on the conformational stability, molecular structure and vibrational spectra of 7-acetoxy-6-(2,3-dibromopropyl)-4,8-dimethyl -coumarin molecule. *J. Mol. Struct.*, 964, 2010, pp.134–151.

[48] Balamurugan, N. Charanya, C. SampathKrishnan, S. Muthu, S. Molecular structure, vibrational spectra, first order hyper polarizability, NBO and HOMO–LUMO analysis of 2-amino-5-bromo-benzoic acid methyl ester, *Spectrochimica Acta Part A: Molecular and Biomolecular Spectroscopy*, 137, (2015), pp. 1374–1386.